Journal of Physics: Conference Series

PAPER • **OPEN ACCESS**

Neutron-Induced Radiation Damage in BaF_2, LYSO/LFS and PWO Crystals

To cite this article: Chen Hu *et al* 2019 *J. Phys.: Conf. Ser.* **1162** 012020

IOP Conf. Series: Journal of Physics: Conf. Series 1162 (2019) 012020 doi:10.1088/1742-6596/1162/1/012020

Neutron-Induced Radiation Damage in BaF_2, LYSO/LFS and PWO Crystals

Chen Hu, Fan Yang, Liyuan Zhang, Ren-Yuan Zhu
California Institute of Technology, Pasadena, CA 91125, USA

Jon Kapustinsky, Michael Mocko, Ron Nelson, Zhehui Wang
Los Alamos National Laboratory, Los Alamos, NM 87545, USA

E-mail: zhu@hep.caltech.edu

Abstract. One crucial issue for applications of inorganic scintillators in future HEP experiments is radiation damage in a severe radiation environment, such as the HL-LHC. While radiation damage induced by ionization dose is well understood, investigations are on-going to understand radiation damage induced by hadrons, including both charged hadrons and neutrons. Aiming at understanding neutron induced radiation damage in fast inorganic scintillators, BaF_2, LYSO/LFS and PWO crystals were irradiated at LANSCE by a combination of particles, including neutrons, protons and γ-rays. The results indicate that LYSO/LFS and BaF_2 crystal plates are radiation hard up to 4×10^{15} fast neutrons/cm^2.

1. Introduction

Because of their superb energy resolution and detection efficiency, crystal scintillators are widely used in high energy physics (HEP) experiments. Fast inorganic crystal scintillators are required by future HEP experiments at the energy and intensity frontiers. One crucial issue, however, is the radiation damage in severe radiation environment expected in future HEP experiments at e.g. the high luminosity large hadron collider (HL-LHC). With a 5×10^{34} cm^{-2}s^{-1} luminosity and a 3,000 fb^{-1} integrated luminosity, the HL-LHC will present a radiation environment, where up to 130 Mrad ionization dose, 3×10^{14} charged hadrons/cm^2 and 5×10^{15} fast neutron/cm^2 are expected [1]. While ionization dose causes a dose rate dependent damage in lead tungstate ($PbWO^4$ or PWO) [2], cumulative damage in PWO was observed by charged hadrons [3, 4].

Bright, fast and radiation hard cerium doped lutetium yttrium oxyorthosilicate ($Lu_{2(1-x)}Y_{2x}SiO_5$:Ce or LYSO) crystals were proposed to construct an LYSO/W/Quartz capillary sampling calorimeter for the CMS upgrade [5], total absorption calorimeters for the SuperB experiment [6] and the Mu2e experiment at Fermilab [7]. They are currently being used to construct a total absorption calorimeter for the COMET experiment at KEK [8], and a 3D calorimeter for the HERD experiment in space [9]. They are also proposed to construct a precision minimum ionization particle (MIP) timing detector (MTD) for CMS Phase-II upgrade for the HL-LHC [10].

One of the reasons for LYSO not being chosen for some HEP experiments is its high cost related to its high melting point and high raw material cost. Alternative cost-effective fast crystals are under investigation. Because of its fast scintillation at 220 nm with sub-nanosecond decay time, barium fluoride (BaF_2) crystals were proposed to construct the Mu2e experiment at Fermilab [11], but were replaced by undoped CsI crystals mainly due to the large intensity of its slow scintillation component with 600 ns decay time [12]. Recent progress in slow component suppression by yttrium doping [13] brings this material back for the proposed Mu2e-II experiment [14].

In this paper, we report neutron induced radiation damage in BaF_2, LYSO and PWO crystals irradiated by a combination of particles, including neutrons, protons and γ-rays at the Weapons Neutron Research facility of Los Alamos Neutron Science Center (WNR of LANSCE) with a fast neutron (>1 MeV) fluence up to 4×10^{15} n/cm^2, a proton fluence up to 1×10^{13} p/cm^2 and several Mrad of ionization dose. Optical and scintillation properties of crystal samples were measured at Caltech HEP crystal lab before and after irradiations. Their applications for future HEP experiments are discussed.

2. Experiments and Samples

Two neutron irradiation experiments 6991 and 7332 were carried out in 2015 and 2016 respectively at the East Port of LANSCE. Fig. 1 shows the Target-4 experiment site of LANSCE (Left) and the East Port (Right). Crystal samples were at about 1.2 m away from the neutron production target.

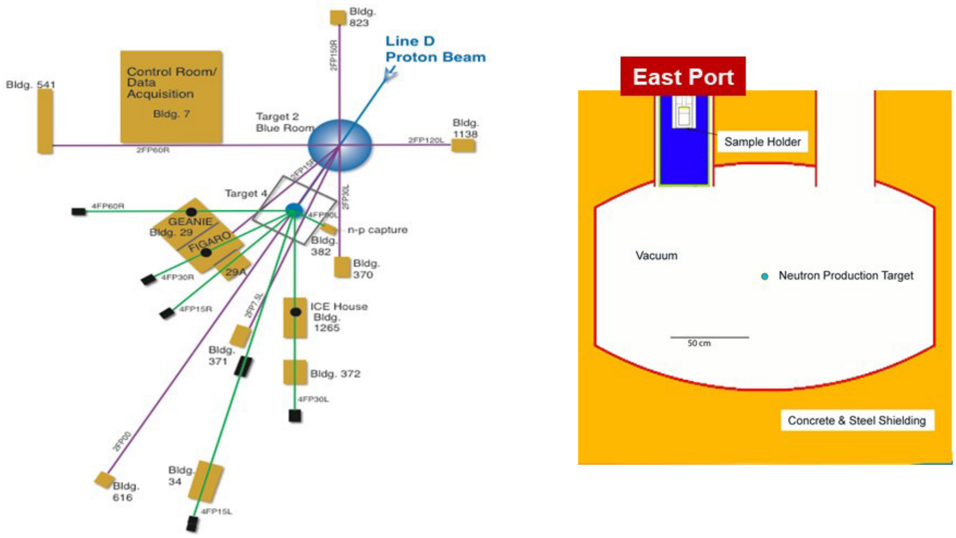

Figure 1. Two schematics showing the neutron irradiation experiment site in the Target 4 area at the center of LANSCE (Left), and the sample location at the East Port (Right).

Fig. 2 shows the particle production rate per incident 800 MeV proton hitting the target as a function of the particle energy for neutrons, protons and photons from 10^{-9} to 10^3 MeV, tallied on the sample volume (averaging) around the samples. These rates are calculated by using a Monte Carlo N-Particle eXtended (MCNPX) transport package developed by LANL [15]. Samples at the East Port were irradiated by a combination of neutrons, protons and photons in these experiments.

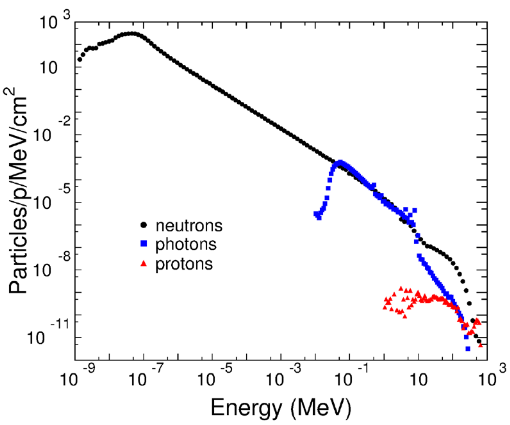

Figure 2. Particle production rate per 800 MeV proton hitting target is shown as a function of particle energy.

Figure 3 Three bars with LFS plates (Left) and the sample holder (Right) for the exp. 6991.

In the experiment 6991, a total of 18 LFS (lutetium fine silicate which is identical to LYSO in performance) crystal plates of 14×14×1.5 mm^3 from Zecotek Photonics Inc. were irradiated. They were divided into three groups of six each. Fig. 3 (Left) shows three groups of LFS samples attached to plastic bars inserted in a sample holder shown at the right. These three groups were down loaded together into the East Port before irradiation, and were retrieved one at a time after 13.4, 54.5 and 118 days. Fig. 4 shows the hourly average current history of the 800 MeV proton beam for the experiment 6991, as well as the retrieving time for three groups. Neutron, proton and photon fluences are calculated by using the particle production rates shown in Fig. 2 integrated over the proton beam current for each group. Table 1 lists the integrated particle fluences for fast neutrons (>1 MeV), very fast neutrons (>20 MeV), protons (>1 MeV) and photons for three groups, the fast neutron fluences are 4.1, 18.6 and 39.3 ×10^{14} n/cm^2 for these three groups.

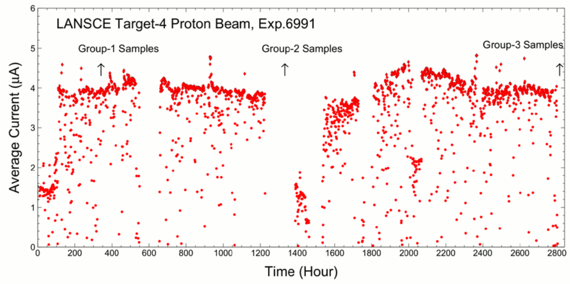

Figure 4. Current history of 800 MeV protons for the exp. 6991.

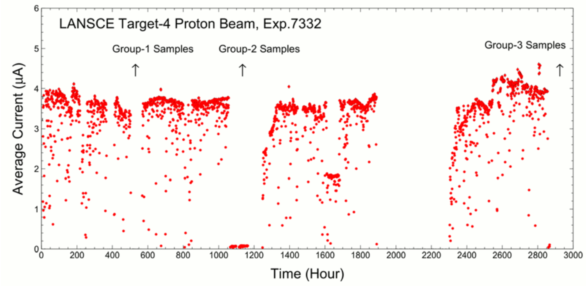

Figure 5. Current history of 800 MeV protons for the exp. 7332.

Table 1 Integrated particle fluences and dose for the LFS plates irradiated in the experiment 6991

Particles	Group-1 Fluence (cm^{-2})	Group-2 Fluence (cm^{-2})	Group-3 Fluence (cm^{-2})
Thermal and Epithermal Neutrons (0 < En < 1 eV)	1.01×10^{15}	4.62×10^{15}	9.76×10^{15}
Slow and Intermediate Neutrons (1 eV < En <1 MeV)	3.67×10^{15}	1.69×10^{16}	3.56×10^{16}
Fast Neutron Fluence (En > 1 MeV)	4.05×10^{14}	1.86×10^{15}	3.93×10^{15}
Very Fast Neutron Fluence (En > 20 MeV)	7.73×10^{13}	3.55×10^{14}	7.50×10^{14}
Proton Fluence (Ep > 1 MeV)	1.18×10^{12}	5.42×10^{12}	1.15×10^{13}
Photon Fluence (Eg > 10 KeV)	1.71×10^{15}	7.88×10^{15}	1.66×10^{16}

Table 2 Integrated particle fluences and dose for the LFS plates irradiated in the experiment 7332

Particles	Group-1 Fluence (cm^{-2})	Group-2 Fluence (cm^{-2})	Group-3 Fluence (cm^{-2})
Thermal and Epithermal Neutrons (0 < En < 1 eV)	1.83×10^{15}	3.96×10^{15}	8.87×10^{15}
Slow and Intermediate Neutrons (1 eV < En <1 MeV)	6.67×10^{15}	1.44×10^{16}	3.23×10^{16}
Fast Neutron Fluence (En > 1 MeV)	7.38×10^{14}	1.60×10^{15}	3.58×10^{15}
Very Fast Neutron Fluence (En > 20 MeV)	1.41×10^{14}	3.04×10^{14}	6.81×10^{14}
Protons Fluence (Ep > 1 MeV)	2.15×10^{12}	4.65×10^{12}	1.04×10^{13}
Photon Fluence (Eg > 10 KeV)	3.12×10^{15}	6.75×10^{15}	1.51×10^{16}

In the experiment 7332, 36 LYSO, BaF_2 and PWO plates of 5 mm thickness were divided into three groups of 12 each, which were irradiated for 21.2, 46.3 and 120 days respectively. Fig. 5 shows the hourly average current history of the 800 MeV proton beam for the experiment 7332. Table 2 lists the integrated particle fluences received by each sample group. The fast neutron (>1 MeV) fluences are 7.4, 16.0 and 35.8 × 10^{14} n/cm^2 for three groups. All crystal samples were produced by Shanghai Institute of Ceramics (SIC). To investigate contributions from ionization dose, 5 mm lead shielding was applied to a half of the samples. In each group, a half of the samples were placed inside a capsule with 5 mm thick Pb wall as shown in Fig. 6 (Top), where a 3D sketch of a plastic sample holder with three chambers (Right) and its cross-section (Left) are also shown. This lead shielding reduced the ionization dose by about 30% integrated over the γ-ray spectrum, but did not affect the fast neutron fluence.

Fig. 7 shows photos taken after irradiation for four each of the LYSO, BaF_2 and PWO plates in the group 3. While the left two samples were shielded by 5 mm Pb, the right two were not. Also shown in the photos is the dimension of these samples. It is 15 × 15 × 5 mm^3 for BaF_2 and PWO, and 10 ×10 × 5 mm^3 for LYSO. While LYSO and BaF_2 samples remained transparent after irradiation, PWO turned black.

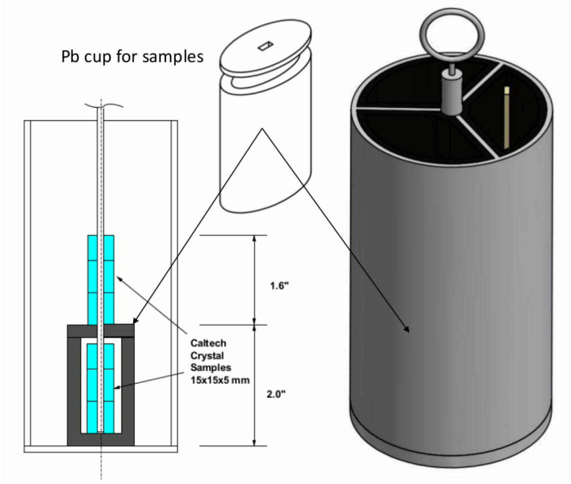

Figure 6. A 3D sketch of the sample holder with three chambers (Right) and its cross-section (Left) showing samples in one chamber, where a half of the samples at the bottom are shielded by 5 mm Pb and the another half of the samples are not.

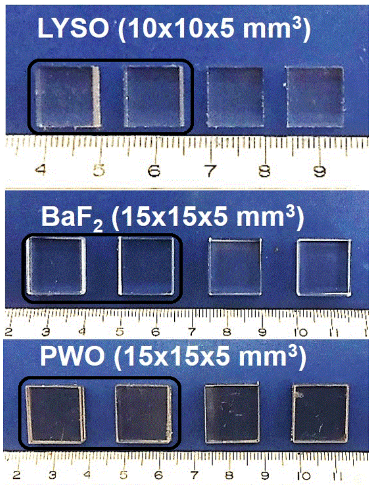

Figure 7. LYSO, BaF_2 and PWO samples with (left two samples) and without (right two samples) 5 mm Pb shielding from the Group-3 after irradiation with particle dose/fluence listed in Table 2.

Emission spectrum of the samples was measured by using an Edinburgh Instruments FLS920 spectrometer. Transmittance spectrum was measured by using a PerkinElmer Lambda 950 spectrophotometer with 0.15% precision. Radiation induced absorption coefficient (RIAC) was calculated as

$$RIAC = \frac{1}{l}\ln\left(\frac{T_0}{T_1}\right) \qquad (1)$$

where l is crystal length, T_0 and T_1 are the transmittances before and after irradiation respectively. The precision of the RIAC values is about 3.5 m^{-1} and 1 m^{-1} for 1.5 mm and 5 mm thick samples respectively [16]. In addition, emission weighted longitudinal transmittance (EWLT) was also calculated,

$$EWLT = \frac{\int T(\lambda)Em(\lambda)d\lambda}{\int Em(\lambda)d\lambda} \qquad (2)$$

where $T(\lambda)$ and $Em(\lambda)$ are transmittance and emission spectra. The EWLT value provides a numerical representation of the transmittance over the entire emission spectrum.

In the experiment 6991, the LFS plates were used in an LYSO/quartz capillary Shashlik calorimeter, so have five holes to allow four Y-11 wavelength shifting (WLS) readout fibers and one central quartz monitoring fiber going through [5]. The light output (LO) of these LFS plates was monitored by a Hamamatsu photomultiplier tube (PMT) R2059 coupled to four Y-11 fibers as shown in Fig. 8. Monitoring light signal generated by a UV LED of 365 nm was injected through the quartz monitoring fiber to excite the LFS plate which was surrounded by a Teflon reflector. A lock-in amplifier was used to mitigate the residual phosphorescence in the samples after irradiation. The monitoring signal measures variations of the LFS response, including light production in both the crystal and Y-11 fibers. The calibration of the entire system was maintained by measuring two reference LFS plates before each measurement. The systematic uncertainty of this monitoring signal measurement was estimated to be about 2.5% by repeated measurements for one reference sample [16].

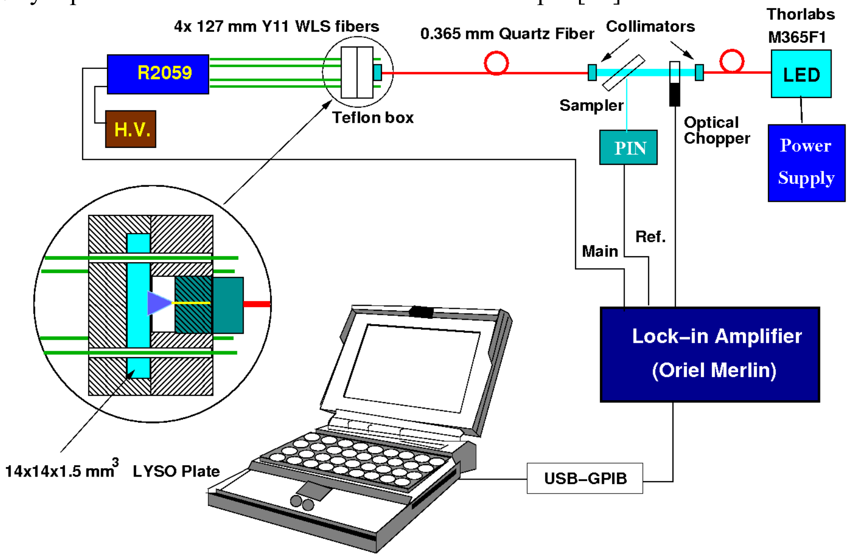

Figure 8. A schematic showing the monitoring setup used to LFS plates in the exp. 6991.

In the experiment 7332, the LO of 5 mm thick LYSO samples before and after irradiation was measured by a Hamamatsu R1306 PMT with a grease coupling for 0.662 MeV γ-rays from a ^{137}Cs source. The LO of BaF_2 and PWO thin plates before and after irradiation was measured by a Hamamatsu R2059 PMT with a grease coupling for 0.511 MeV γ-rays from a ^{22}Na source with a coincidence trigger. The systematic uncertainty of these measurements is about 1%.

3. Experimental Results

3.1 LFS Plates in the experiment 6991

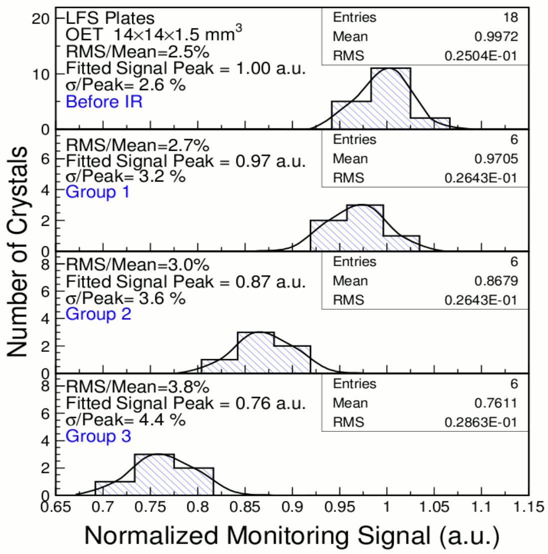

Figure 9. Monitoring signal measured before irradiation for all LFS plates, and after irradiation.

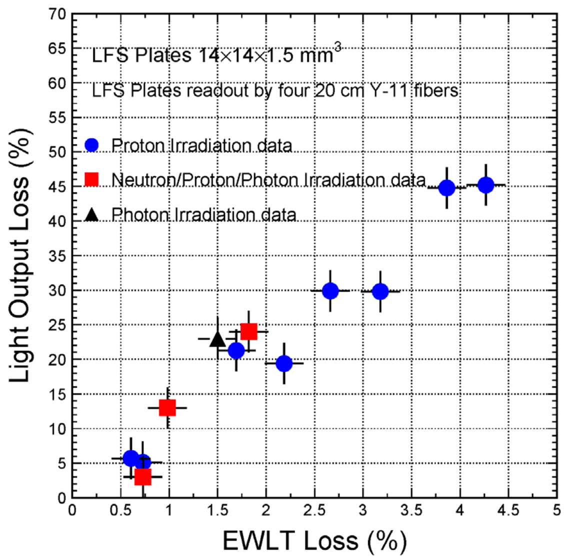

Figure 10. Normalized monitoring signal is shown as a function of EWLT for LFS plates after irradiation.

Both the monitoring signal and transmittance were measured for LFS plates before and after irradiations. Fig. 9 shows the normalized monitoring signal measured before irradiation for all samples and after irradiation for the three LFS plate groups. The top plot shows that the LFS plates have consistent monitoring signal intensity before irradiation with a dispersion of 2.5% consistent with the systematic uncertainty. The monitoring signal after irradiation was normalized to their corresponding values before irradiation for each plate. Average losses of 3, 13 and 24% are observed. The corresponding EWLT losses are 0.6, 1.1 and 1.8% for these three groups.

Fig. 10 shows the normalized monitoring signal measured with four Y-11 WLS fibers as a function of the EWLT loss for the LFS plates irradiated in the experiment 6991 (red squares), and compared to LFS plates of the same dimension irradiated by Co-60 γ-rays at JPL (black triangle) as well as 24 GeV protons at CERN (blue dots). The data shown in this figure are the average of a number of samples irradiated under the same condition. We notice a consistent correlation between the LO (monitoring signal) losses and the EWLT losses for samples irradiated by various sources, indicating that the radiation damage induced by protons, neutrons and photons in LFS plates may be corrected for by an optical monitoring system.

To observed damage is caused by fast neutrons, protons and photons. The proton fluence is more than 300 times lower than that of the fast neutrons. According to the data obtained in the proton irradiation experiment at LANL with 800 MeV protons [16], the contribution from such a fluence is known to be less than 0.1 m^{-1} in the experiment 6991. The ionization dose, however, is estimated to be at Mrad level, which would cause damage in these crystals [17]. To understand γ-ray contribution, 5 mm lead shielding was applied to a half of the samples in the experiment 7332 in 2016. The 5 mm Pb reduced γ-rays induced ionization does by 30%, but did not affect the fast neutron fluence.

3.2 LYSO, BaF_2, and PWO plates in the experiment 7332

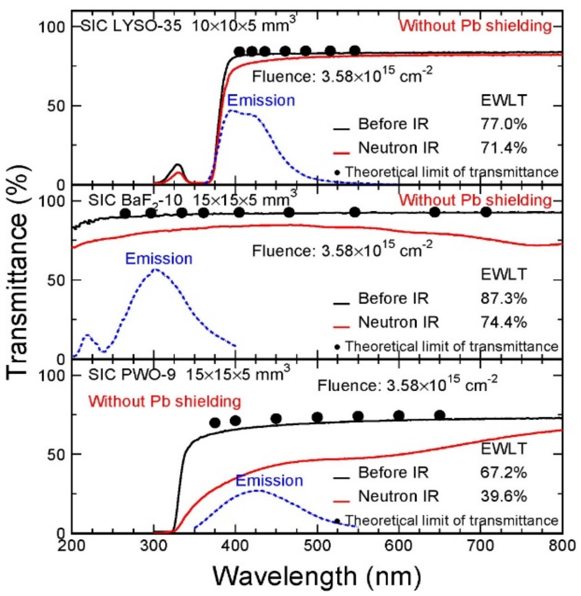

Figure 11. Transmittance spectra for one sample each of LYSO (top), BaF_2 (middle) and PWO (bottom) without Pb shielding before and after irradiation.

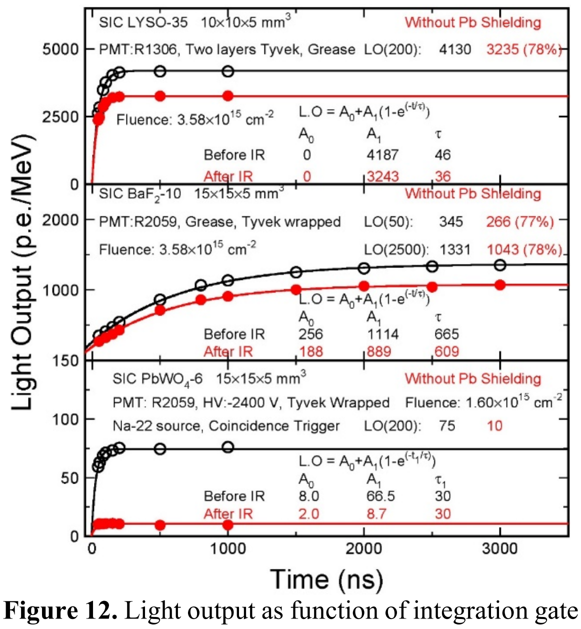

Figure 12. Light output as function of integration gate for one sample each of LYSO (top), BaF_2 (middle) and PWO (bottom) without Pb shielding before and after irradiation.

Fig. 11 shows transmittance spectra before and after irradiation for one sample each of LYSO (top), BaF_2 (middle) and PWO (bottom) without Pb shielding in the group 3. Also shown in the figure are the corresponding theoretical limit of transmittance (black dots) for each crystal calculated by using crystal's refractive index assuming multiple bounces and no internal absorption [18]. Excellent optical quality was observed in these samples before irradiation. Also listed in the figure are the numerical values of EWLT, which are 71.4%, 74.4%, and 39.6% respectively for SIC LYSO, BaF_2, and PWO after a fast neutron fluence of $3.6\times10^{15}/cm^2$. These data explain the color observed in PWO samples in Fig. 7, and indicate a much better radiation resistance of LYSO and BaF_2 than PWO.

Fig. 12 shows the LO as a function of the integration time for LYSO, BaF_2, and PWO samples without Pb shielding before and after irradiation. While both LYSO and BaF_2 samples showed a LO degradation of about 22% after a fast neutron fluence of $3.6\times10^{15}/cm^2$ (group 3), about 86% loss in LO is observed in PWO after a fast neutron fluence of $1.6\times10^{15}/cm^2$ (group 2). We also note, the degradation in LO for LYSO crystals is consistent with the 25% loss observed in the LFS plates with ELS fiber readout in the experiment 6991. The LO of PWO in group 3 was too low to be measured.

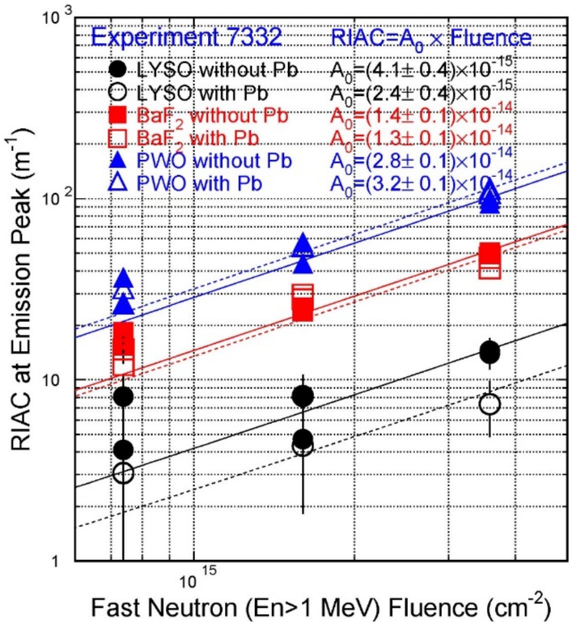

Figure 13. The RIAC values are shown as a function of the fast neutron fluence for six each of LYSO, BaF_2 and PWO plates.

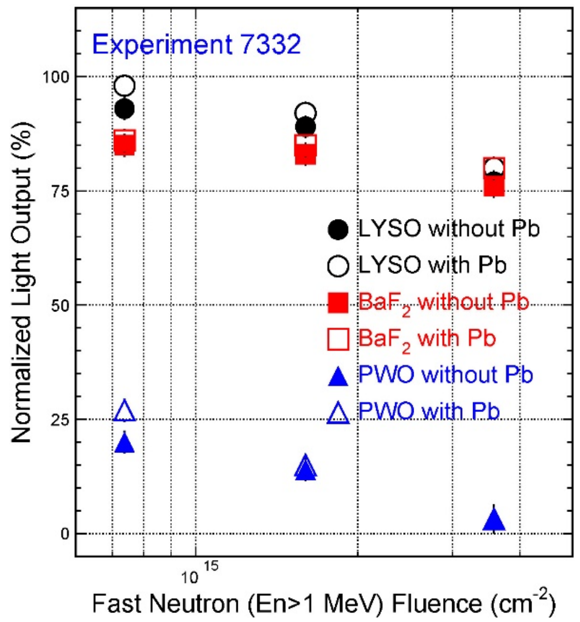

Figure 14. The normalized LO is shown as a function of the fast neutron fluence for LYSO, BaF_2 and PWO plates.

Fig. 13 shows the RIAC values at the corresponding emission peak as a function of the fast neutron (> 1 MeV) fluence for six each of LYSO (circles), BaF_2 (squares) and PWO (triangles) crystals with (open) and without (solid) lead shielding, and the corresponding fits. While the average RIAC values are 14.1, 49.8 and 110.5 m^{-1} respectively for LYSO, BaF_2 and PWO without 5 mm Pb shielding, the corresponding values are 7.3, 44.2 and 97.1 m^{-1} with Pb shielding. The Pb shielding thus indeed reduced the damage level, hinting that γ-ray induced damage is not negligible. It, however, is difficult to quantitatively subtract the contribution of photon ionization dose because of uncertainties in dose calibration and sample to sample variation. The results presented here thus may be considered as an upper limit of neutron induced damage. Additional works are needed to reach a quantitative conclusion for radiation damage induced by ionization dose, protons and neutrons.

Fig. 14 shows the normalized LO as a function of the fast neutron fluence for LYSO, BaF_2 and PWO. Each LO value is the average of two samples irradiated with the same condition. The normalized LO values are 77% and 76% respectively for LYSO and BaF_2 crystals without Pb shielding, and 80% and 80% with Pb shielding. In both cases, the LO of PWO samples in the group 3 is too low to be measured in the lab after neutron (>1 MeV) fluence of 3.6×10^{15} n/cm^2. The data point for the PWO crystals in the group 3 thus indicates an upper limit. It is clear that LYSO and BaF_2 are much more radiation hard than PWO under neutron irradiations.

4. Summary

LFS, BaF_2, LYSO and PWO crystal plates were irradiated by a combination of neutrons, protons and γ-rays at the East Port of LANSCE in two experiments: 6991 in 2015 and 7332 in 2016. In both experiments, samples were arranged in three groups to receive a fast neutron fluence up to 4×10^{15} n/cm^2. The observed LO losses at a level of <25% were observed for LYSO and BaF_2 crystals of 10 × 10 × 5 mm^3 after a fast neutron (>1 MeV) fluence of 3.6×10^{15}/cm^2, indicating that they are promising materials to be used in a severe radiation environment, such as the HL-LHC. A 5 mm lead shielding applied to a half of the samples in the experiment 7332 showed evident contribution of ionization dose induced damage. We plan to continue this investigation to reach quantitative conclusions on hadron induced radiation damage in inorganic scintillators.

Acknowledgments

This work was supported in part by the US Department of Energy Grants DE-SC0011925 and DE-AC52-06NA25396.

References

[1] B. Bilki on behalf of the of the CMS Collaboration, "CMS Forward Calorimeters Phase II Upgrade," J. Phys.: Conf. Ser. 587(1), pp. 012014 (2015).
[2] R.-Y. Zhu, "The Next Generation of Crystal Detectors," J. Phys.: Conf. Ser. 587(1), pp. 012055 (2015).
[3] M. Huhtinen, P. Lecomte, D. Luckey, F. Nessi-Tedaldi, F. Pauss, "High-energy proton induced damage in PWO calorimeter crystals," Nucl. Instr. Meth. Phys. Res. A 545(1), pp. 63-87 (2005).
[4] R.-Y. Zhu, "A Comparison of Monitoring Data with Radiation Damage in PWO Crystals by Ionization Dose and Charged Hadron," http://www.hep.caltech.edu/~zhu/talks/ryz_ 161028_ PWO_mon.pdf.
[5] L. Y. Zhang, R. H. Mao, F. Yang, R.-Y. Zhu, "LSO/LYSO Crystals for Calorimeters in Future HEP Experiments," IEEE Trans. Nucl. Sci. 61, pp. 483-488 (2014).
[6] G. Eigen, Z. Zhou, D. Chao, et al., "A LYSO calorimeter for the SuperB factory," Nucl. Instr. Meth. Phys. Res. A 718(c), pp. 107-109 (2013).
[7] G. Pezzullo, J. Budagov, R. Carosi, et al., "The LYSO crystal calorimeter for the Mu2e experiment," J. Instrum. 9(3), pp. C03018 (2014).
[8] K. Oishi, "An LYSO Electromagnetic Calorimeter for COMET at J-Park," paper O47-4 presented in IEEE NSS2014, Seattle, 8-15 Nov 2014.
[9] S.N. Zhang, O. Adriani, S. Albergo, et al., "The High Energy cosmic-Radiation Detection (HERD) Facility onboard China's Future Space Station," Proc. SPIE Int. Soc. Opt. Eng. 9144, pp. 91440X (2014).
[10] T. Tabarelli de Fatis., "Precision timing studies and detector concept proposal," presentation given in the CMS general meeting, 16 Nov 2016.
[11] G. Pezzullo, J. Budagov, R. Carosi, et al., "Progress Status for the Mu2e Calorimeter System," J. Phys.: Conf. Ser. 587(1), pp. 012047 (2015).
[12] S. Miscetti on behalf of the Mu2e calorimeter group, "Design and status of the Mu2e crystal calorimeter,"https://indico.cern.ch/event/88511/contributions/2612678/attachments/1537319/2409090/M_2_4_MU2EEMC_SCINT.pdf
[13] R.-Y. Zhu, "Applications of Very Fast Inorganic Crystal Scintillators in Future HEP Experiments," in Proceedings of the TIPP 2017 conference, Beijing, China, http://www.hep.caltech.edu/~zhu/talks/ryz_170522_Fast_Crystals.pdf
[14] The Mu2e Collaboration, "Expression of Interest for Evolution of the Mu2e Experiment," https://mu2e-docdb.fnal.gov/cgi-bin/private/ ShowDocument?docid=10655
[15] MCNPX User's Manual, version 2.7.0, Denise B. Pelowitz (editor), April 2011, LA-CP-11-00438
[16] F. Yang, L. Zhang, R.-Y. Zhu, J. Kapustinsky, R. Nelson and Z. Wang, "Proton-Induced Radiation Damage in Fast Crystal Scintillators," IEEE Trans. Nucl. Sci. 64, pp. 665-672 (2017).
[17] F. Yang, L. Zhang, R.-Y. Zhu, "Gamma-Ray Induced Radiation Damage Up to 340 Mrad in Various Scintillation Crystals," IEEE Trans. Nucl. Sci. 63, pp. 612-619 (2016).
[18] R. Mao, L. Zhang, R.-Y. Zhu, "Optical and Scintillation Properties of Inorganic Scintillators in High Energy Physics," IEEE Trans. Nucl. Sci. 55, pp. 2425-2431 (2008).